

OMAE2012-8' % -

WIND EFFECT ESTIMATION IN SIDE BY SIDE OFFLOADING OPERATION FOR FLNG AND LNG CARRIER SHIPS

Toshifumi Fujiwara

Ocean Engineering Department

Kazuhiro Yukawa

Ocean Engineering Department

Hiroshi Sato

Ocean Engineering Department

Kazuhisa Otsubo

Ocean Engineering Department

Tomoki Taniguchi

Ocean Engineering Department

National Maritime Research Institute
Mitaka, Tokyo, 1810004, JAPAN

ABSTRACT

Liquid Natural Gas resource development is often conducted worldwide. Recently the drilling area has gradually expanded from shallow sea area to the deep ocean. A Floating LNG facility (FLNG) and a LNG carrier ship (LNG) are assumed to operate in the open sea expected to wind, wave and current. In this situation, an operational capability evaluation of the LNG would be needed to grasp the operational weather limitation. The effect of each weather element, i.e. wind, wave and current, giving manoeuvring effect to ships, is expected to assess exactly as external loads. In such a situation, wind interaction effect under the operating condition that a FLNG and a LNG are in same closed area is not clearly understood. This paper treats and proposes one estimation method of wind load for the operation of side-by-side offloading including interaction effect of a FLNG and a LNG. The proposed wind load estimation method based on the wind tunnel experiments represents the shielding effect of the LNG behind the FLNG. Operational assessment on ship manoeuvring under strong wind is calculated using the proposed wind load method in the final stage.

1 INTRODUCTION

The LNG offloading critical limitation under rough sea is important information for the operation of transferring storage LNG resource from a Floating LNG facility (FLNG) to a LNG carrier ship (LNG). The side by side offloading operation, see Figure 1, to supply liquid gas from the FLNG to the LNG is adopted frequently with easier operational reason rather than

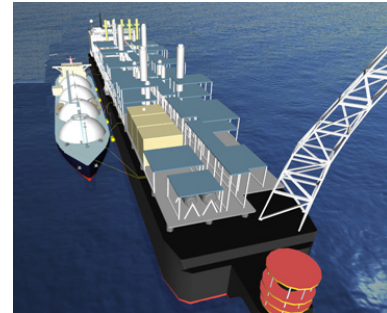


Figure 1. Image example picture in case of side by side offloading operation of FLNG & LNG.

tandem style operation. In the side by side offloading operation, however, weather conditions must be monitored enough to prevent the collision accident between the FLNG and the LNG.

In this paper, the authors have focused the wind shielding effect in side by side offloading situation of operating ships. In the past presented papers by the other authors [1]~[4], general information noted the importance of consideration for the wind shielding effect was pointed out, and in some cases, CFD (Computational Fluid Dynamics) calculations in the ship shielding conditions was conducted[4]. Detail analysis of the effect based on experimental or the wind shielding effect on calculated results, however, have not generally been presented in them. An easier estimation method or logic of the effect on

Table 1. Principal particulars of the sample ships on fully loaded FLNG and ballasted LNG (1/200 models).

FLNG (Full)				LNG (Ballast)			
	Unit	Ship	Model		Unit	Ship	Model
L_{OA}	m	336.0	1.680	L_{OA}	m	289.5	1.448
L_{PP}	m	328.6	1.643	L_{PP}	m	277.0	1.385
B	m	50.0	0.250	B	m	49.0	0.245
D	m	31.6	0.158	D	m	27.0	0.135
d	m	12.2	0.061	d	m	9.4	0.047
A_F	m ²	2482	0.062	A_F	m ²	1885	0.047
A_L	m ²	10126	0.253	A_L	m ²	8855	0.221
A_{OD}	m ²	4200	0.105	A_{OD}	m ²	4087	0.102
C	m	-3.4	-0.017	C	m	-3.7	-0.019
H_C	m	19.7	0.099	H_C	m	15.3	0.077
H_B	m	46.2	0.231	H_B	m	47.3	0.237

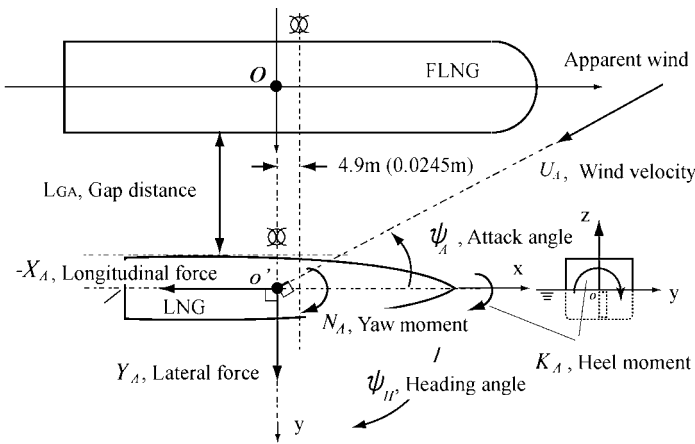


Figure 2. Coordinate system of wind force coefficients and basic positioning relation between FLNG and LNG.

ship shielding conditions is expected for operational risk from the viewpoints of practical use.

Then an attempt on wind load estimation method for a LNG with the shielding effect is presented in this paper.

Initially, the wind tunnel experiments for a FLNG and a LNG models in the side by side situation are presented. The experiments were carried out in our research institute in order to grasp aerodynamic specification for those models. Many kinds of positions for the FLNG and the LNG were set in the experiments.

Secondly, using those experimental results, some aerodynamic specific theories are clarified, and it is shown that the estimation method for wind load, including the shielding effect, can be applied to the ships in side by side situation and approaching. This method is simply based on the geometrical ship position and external form.

Finally, the shielding effect on the FLNG-LNG carrier ships operation is also shown using the ship manoeuvring simulation in wind. The calculated results for the LNG drift

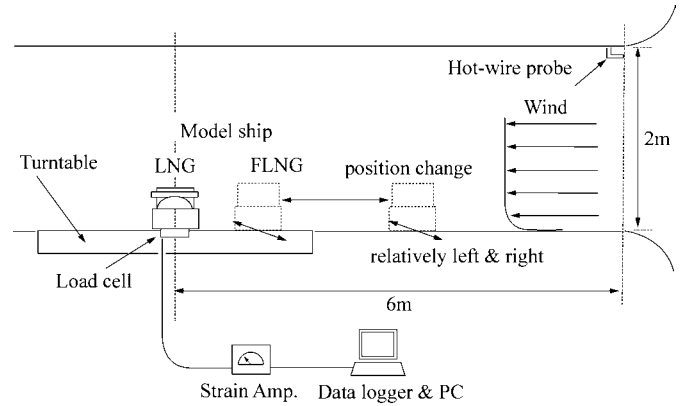


Figure 3. Experimental setup in the wind tunnel.

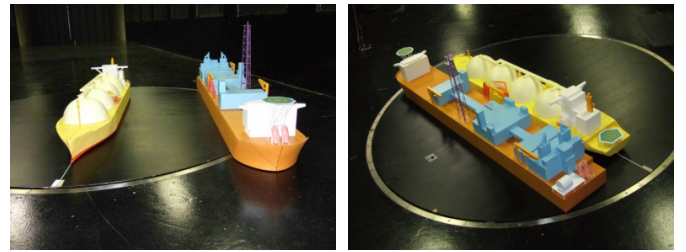


Figure 4. Photos of experimental conditions in the wind tunnel.

motion present the importance of the evaluation of the FLNG shielding effect to estimate the operational risk on side by side situation.

2 WIND FORCE EXPERIMENTS

2.1 SAMPLE SHIPS:

The sample ships, a FLNG and a LNG, shown in Table 1 are used in the experiments and calculations in this paper. Here in the table, L_{OA} ; the overall length, L_{PP} ; the length between perpendiculars, B ; the breadth, D ; the draught, d ; the depth, A_F ; the frontal projected area, A_L ; the lateral projected area and A_{OD} ; the lateral projected area of superstructure etc. on the deck. Moreover, C ; the horizontal distance from amidships section to center of lateral projected area, H_C ; the height from calm water surface to center of lateral projected area, H_B ; the height of top of superstructure (bridge etc.) are included in the table. These ships are typical size of the gas loading operation. A moss type LNG ship with 4 large spherical tanks on the deck is studied.

2.2 COORDINATE SYSTEM OF WIND FORCES:

The wind shielding effect in side by side offloading situation of operating ships is considered. The LNG is in behind the larger FLNG. Figure 2 defines the cartesian x-y coordinate reference system for the wind forces and moments used in the

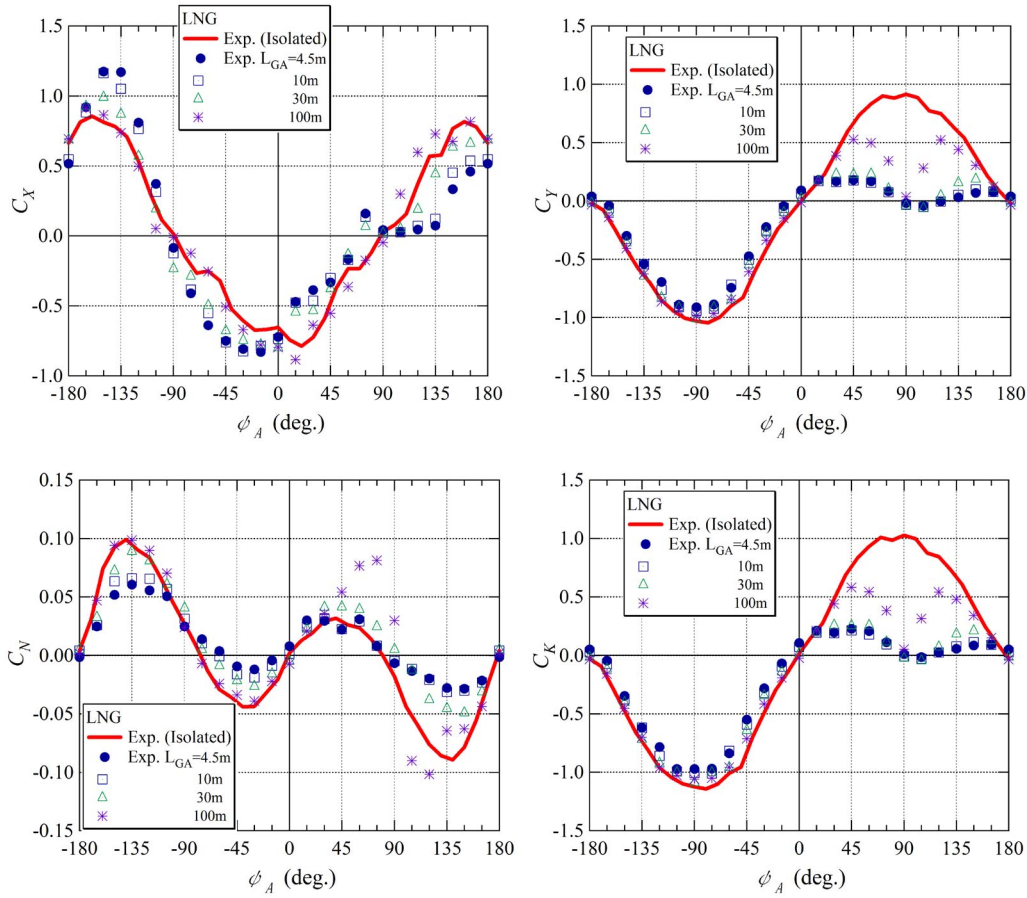


Figure 5. Example of experimental results on longitudinal, lateral forces, C_X & C_Y , and yaw, heel moment, C_N & C_K of LNG

paper and the interrelationship position of the FLNG and the LNG. The origin for the main object, in this case of LNG, is located at the amidship, the still water line, and on the longitudinal line of ship symmetry. Figure 2 also provides definitions and associated sign conventions for the longitudinal force X_A , the lateral force Y_A and the yaw & heel moment N_A , K_A . The apparent angle of attack of the wind relative to the positive x-axis of the ship is defined as ψ_A . The non-dimensional form of the longitudinal & lateral forces and yaw & heel moment are defined as follows:

$$\begin{aligned} C_X(\psi_A) &= X_A(\psi_A)/(q_A A_F) \\ C_Y(\psi_A) &= Y_A(\psi_A)/(q_A A_L) \end{aligned} \quad (1)$$

$$\begin{aligned} C_N(\psi_A) &= N_A(\psi_A)/(q_A A_L L_{OA}) \\ C_K(\psi_A) &= K_A(\psi_A)/(q_A A_L H_L) \\ q_A &= \frac{1}{2} \rho_A U_A^2 \end{aligned} \quad (2)$$

with ρ_A the indicating air density, U_A the apparent wind velocity, H_L ; the mean height of a ship (equal to A_L/L_{OA}).

2.3 EXPERIMENTAL SETUP:

Experimental setup in the wind tunnel is shown in Figure 3. Figure 4 is the experimental condition's photos in the wind tunnel. The wind tunnel experiments were carried out at our institute, NMRI. The tunnel is a Göttingen-type, breadth 3m \times height 2m test section and has ability to make 30m/s wind velocity. The wind velocity selected for the investigations corresponds to a mean value of approximately 24m/s and Reynolds' number of 10^6 order for the model length, where the model is in turbulent flow condition, since the drag coefficients were independent of the Reynolds' number in this region.

2.4 SAMPLE OF EXPERIMENTAL RESULTS:

Figure 5 presents the four forces components of experimental results, longitudinal, lateral forces, C_X & C_Y , yaw, heel moments, C_N & C_K respectively. In the legend, the

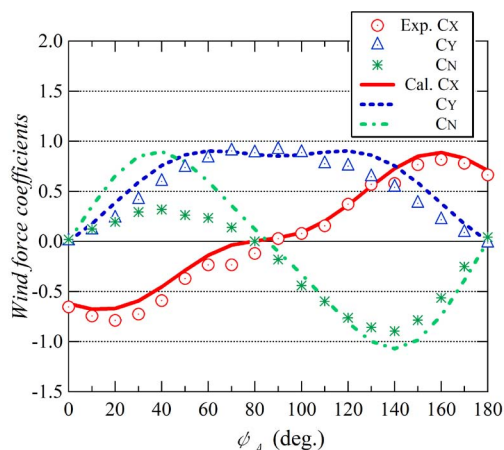


Figure 6. Comparison between the experimental results on wind force coefficients and calculated ones on isolated LNG.

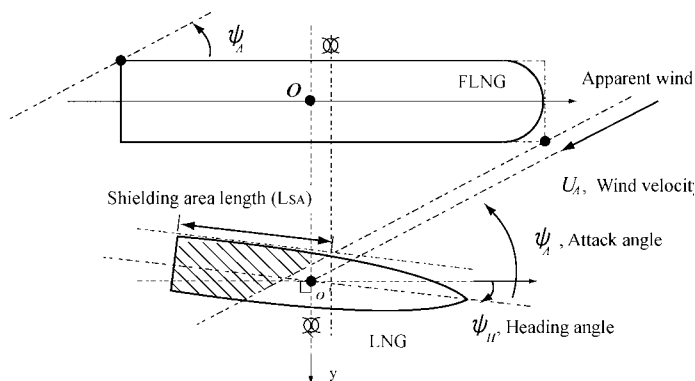


Figure 7. Definition of the shielding area length projected to LNG

L_{GA} value, that means for the gap length as shown in Figure 2, has real ship order. The results of each condition were compared with the isolated LNG experimental results, which are the red line in the figures.

For C_Y & C_K in the $45 < \psi_A < 135$ deg., as the LNG is in the shielding area of the FLNG, the experimental values are rapidly reduced getting closer to behind the FLNG. On the other hand, the C_N has the tendency of increase in the same area by contrast.

The shielding effect shown in the Figure 5 is expressed in the next chapter in considering the wind load estimation method on side by side offloading situation and approaching.

3 WIND FORCES ESTIMATION METHOD CONSIDERED WITH SHIELDING EFFECT

The authors proposed an estimation method of wind force coefficients and moment coefficients for an isolated conventional ship, which has the best accuracy level than

previous methods, using the physical components, namely the longitudinal-flow drag, cross-flow drag, lift and induced drags [5][6]. To estimate wind force and moment coefficients, the 8 basic hull form parameters represented in Table 1, excluding the length between perpendiculars L_{PP} , the draught D , the depth d , are used in the estimation method. The detailed way to estimate wind load is explained in Ref. [5][6]. Figure 6 shows as an example, the calculated results compared with the experimental ones for the LNG. The estimation method proposed by the author has enough accuracy to use in ocean engineering situations, though C_N from 0deg. to 90deg. has a little overestimation values.

Here, the wind load estimation method for a ship including shielding effect on the basis of the previous author's estimation method is explained in the next term. At this time, heel moment study is omitted, as the treat would be easily applied using the lateral force estimation method. And the study subject of the estimation method is limited as the case that the LNG is in the behind the FLNG under wind, that shows the right hand side in the each graph in Figure 5.

3.1 BASIC CONCEPT:

To propose the wind load estimation method including shielding effect, the following assumptions are taken into account for the ship wind load.

- 1) The wind shielding effect is disappeared at $\psi_A = 0$ & 180 deg. in the side by side situation for a FLNG and a LNG
- 2) The wind shielding effect is related to the gap length and the wind shielding area of a ship.

This second assumption was acquired from the wind tunnel experiments on a container ship with several kinds of forms on deck containers [7]. The gap length is defined as L_{GA} in Figure 2. Moreover, the shielding area length for wind direction is decided as L_{SA} shown in Figure 7. The points of reference getting L_{SA} are set at the each corner of a rectangular image form at FLNG outer frame. The LNG's fore and aft position and drift angle against the FLNG influence on the L_{SA} value.

To investigate the accuracy of the assumption of above mentioned second term, that is 2), the experimental results of the lateral force coefficient C_Y are taken up at first.

Figure 8 shows the experimental results on reduced ratio of C_Y that is defined as $\Delta C_Y / C_Y$. For example, in case $L_{GA} / L_{OA} \approx 0.0$, that is near contact situation, C_Y of the LNG becomes near zero value (In this case, the reduced ratio $\Delta C_Y / C_Y$ becomes nearly equal to 1.0.) because of the direct shielding position of the FLNG from wind.

In proportion to be the LNG at outside, reducing shielding situation, $\Delta C_Y / C_Y$ becomes to be zero. In $\psi_A = 90$ deg. the shielding effect of the FLNG remains for long distance of the L_{GA} / L_{OA} . This shielding effect in the case of $\psi_A = 90$ deg. can be considered as the maximum level of ship to ship interaction.

The trend shielding effect of $\psi_A=90\text{deg.}$ is represented as the Gaussian distribution like following coefficient:

$$C_{S1} = \Delta C_Y / C_Y = \exp\left\{-\left(\frac{L_{GA}}{L_{OA}}\right)^2 / 2a_0^2\right\}, \quad a_0 = 1.1 \quad (3)$$

An appropriate line of $\Delta C_Y / C_Y$ depending on L_{GA} / L_{OA} is shown in Figure 8 as a red dashed line.

On the other hand, in the case of the LNG near the side of the FLNG ($L_{GA} / L_{OA}=0.015\sim 0.35$), the ratio L_{SA} / L_{OA} becomes a very important factor for $\Delta C_Y / C_Y$, having also the small level effect of the wind direction, as shown in Figure 9. Generally the trend of the experiments is represented by a high-order function. In the case of Figure 9 result, the effect of the reduction of $\Delta C_Y / C_Y$ is assumed to be multiplied by the quartic function as follow:

$$C_{S2} = \Delta C_Y / C_Y = (L_{SA} / L_{OA})^4 \quad (4)$$

From the results of Figure 8 and Figure 9, it becomes clear that the L_{GA} / L_{OA} and the L_{SA} / L_{OA} have an important role for wind load shielding effect. Then referencing on the relation Eq. (3) and (4) each component of wind force coefficients is considered from next section.

3.2 LONGITUDINAL FORCE COEFFICIENT:

The longitudinal force coefficient, C_X , of the original method [5][6] consists of the longitudinal flow drag, F_{LF}' , lift & drag, F_{XLI}' , caused by the liner potential theory, and additional force caused by the 3-dimensional flow effect, F_{ALF}' , as follows:

$$\begin{aligned} C_X(\psi_A) &= F_{LF}' + F_{XLI}' + F_{ALF}' \\ &= C_{LF} \cos\psi_A \\ &+ C_{XLI} \left(\sin\psi_A - \frac{1}{2} \sin\psi_A \cos^2\psi_A \right) \cdot \sin\psi_A \cos\psi_A \\ &+ C_{ALF} \sin\psi_A \cos^3\psi_A \end{aligned} \quad (5)$$

It is considered that each component in Eq. (3) is also affected by the wind shielding effect. Using the trend of the shielding effect obtained from Section 3.1, the effectiveness term on the shielding effect is added in Eq. (5).

$$\begin{aligned} C_X(\psi_A) &= (1 - a_1 C_{S1} C_{S2}) (F_{LF}' + F_{XLI}' + F_{ALF}') \\ C_{S1} &= \exp\left\{-\left(\frac{L_{GA}}{L_{OA}}\right)^2 / 2a_0^2\right\} \\ C_{S2} &= (L_{SA} / L_{OA}) \end{aligned} \quad (6)$$

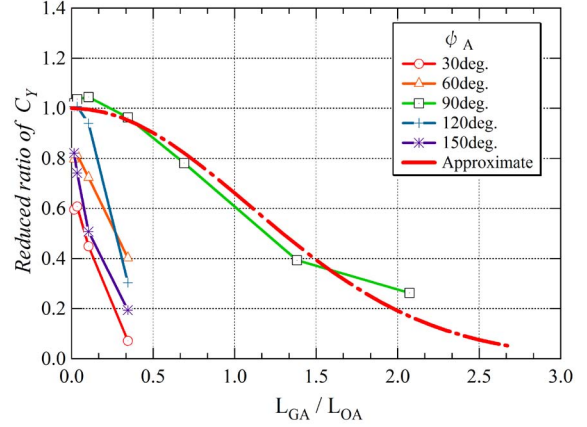


Figure 8. Experimental results of reduced ratio on C_Y and appropriation line of $\Delta C_Y / C_Y$ depending on L_{GA} / L_{OA} .

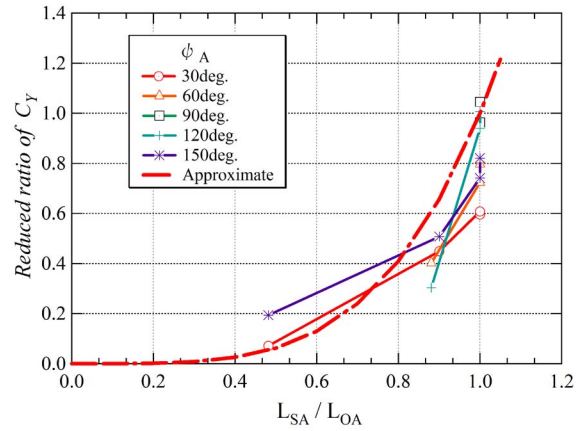


Figure 9. Experimental results of reduced ratio on C_Y and appropriation line of $\Delta C_Y / C_Y$ depending on L_{SA} / L_{OA} . ($L_{GA} / L_{OA}=0.015\sim 0.35$)

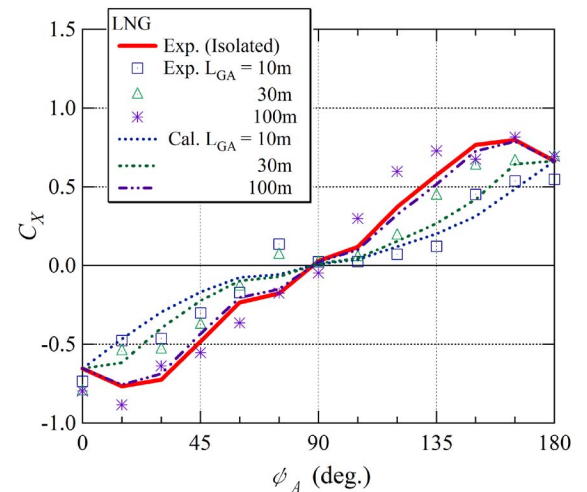


Figure 10. Comparison between the experimental results on C_X and calculated ones.

Here, a_1 and a_2 are chosen as 0.69 and 0.20 respectively to fit the experimental trend. The results are presented in Figure 10 with the experimental results. In order to make decision of a_2 value, it referred that in case $L_{GA} = 100\text{m}$ the shielding effect is mostly vanished in the experimental data.

3.3 LATERAL FORCE COEFFICIENT:

The lateral wind force coefficients C_Y are defined in the original method as follows:

$$\begin{aligned}
 C_Y(\psi_A) &= F'_{CR} + F'_{YLI} \\
 &= C_{CR} \sin^2 \psi_A \\
 &\quad + C_{YLI} \left(\cos \psi_A + \frac{1}{2} \sin^2 \psi_A \cos \psi_A \right) \cdot \sin \psi_A \cos \psi_A
 \end{aligned} \tag{7}$$

Here, F'_{CR}, F'_{YLI} are cross-flow drag, and lift and induced drags in the lateral direction components, respectively. The authors modify Eq. (5) including the shielding effect the same way as the C_X .

As mentioned above, the lateral wind force has relationship L_{GA}/L_{OA} and L_{SA}/L_{OA} ratio. Referencing the Figure 8 and 9, and using the original estimation of Eq. (7), the equation of C_Y including the shielding effect is the following:

$$\begin{aligned}
 C_Y(\psi_A) &= (1 - C_{S3} C_{S4}) (F'_{CR} + F'_{YLI}) \\
 C_{S3} &= \exp \left\{ - \left(\frac{L_{GA}}{L_{OA}} \right)^2 / 2b^2 \right\}, \quad b = 1.1 \\
 C_{S4} &= (L_{SA} / L_{OA})^4
 \end{aligned} \tag{8}$$

Figure 11 shows the comparison between the experimental results on C_Y and calculated ones. The calculated results using Eq. (7) is expressing the experimental results in general.

3.4 YAW MOMENT COEFFICIENT:

The yaw moment coefficients C_N in the original method using the lateral wind force C_Y like these:

$$\begin{aligned}
 C_N(\psi_A) &= C_Y(\psi_A) \cdot L_N(\psi_A) \\
 &= C_Y(\psi_A) \cdot \left[0.927 \times \frac{C}{L_{OA}} - 0.149 \times \left(\psi_A - \frac{\pi}{2} \right) \right]
 \end{aligned} \tag{9}$$

The non-dimensional moment levers L_N are obtained from the experiments like Figure 12. In usual the neighboring $\psi_A = 90\text{deg}$, the levers L_N approaches to zero. However, in shielding cases, wind flows at the ship bow or stern area rather than at the mid-ship. Then the point of application of the wind

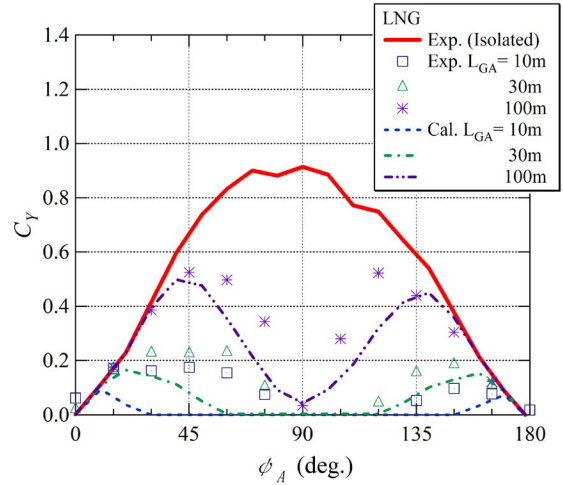


Figure 11. Comparison between the experimental results on C_Y and calculated ones.

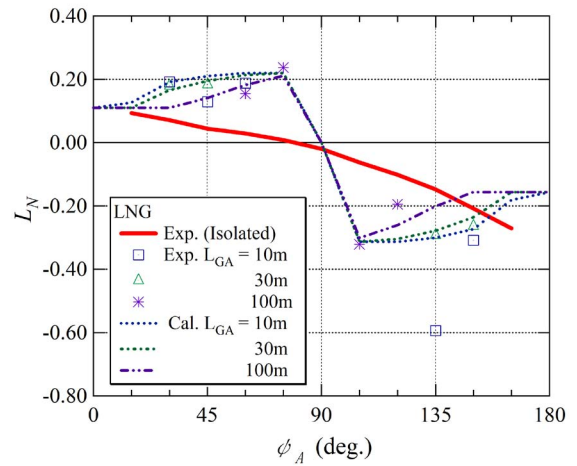


Figure 12. The non-dimensional moment levers L_N comparing experimental results and calculated ones.

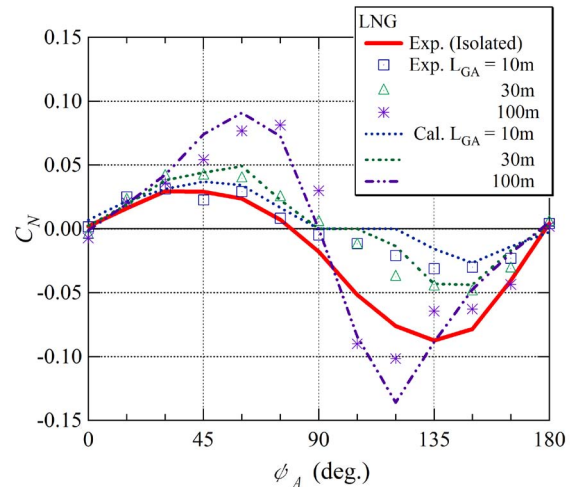


Figure 13. Comparison between the experimental results on C_N and calculated ones.

lateral force places at the spot away from amidship, that means a moment lever becomes larger relatively.

To express the formulation on the C_N , the C_Y is calculated using the lateral force estimation method in Eq. (8) affected by shielding. This is the same way as the original C_N estimation equation Eq. (9). Moreover, the shielding effect to moment lever is added to the original L_N . Considering the L_N formulation, following plans are picked out:

- 1) The force application point of yaw moment works on the center line for breadth and at the center of no shielding area for length direction.
- 2) The trend of the L_N is highly nonlinear in case of $90\text{deg.} < \psi_A < 180\text{deg.}$ The results of short gap length are ignored for expressing the L_N formulation, since the C_N values of those ranges are very small rather than the other cases.

As the final decision, non-dimensional moment lever L_N including shielding effect is expressed as follows:

$$L_N(\psi_A) = L_{N0}(\psi_A) \cdot (1 - C_{S3}) + L_{NS}(\psi_A) \cdot C_{S3} \quad (10)$$

$$L_{NS}(\psi_A) = \pm 0.25 C_{S5} \left(\frac{L_{SA}}{L_{OA}} < 0.5 \right)$$

$$= \pm C_{S5} \frac{L_{SA}}{2L_{OA}} \left(0.5 \leq \frac{L_{SA}}{L_{OA}} \right) \begin{cases} 0 \leq \psi_A \leq \pi/2 \\ \pi/2 \leq \psi_A \leq \pi \end{cases}$$

where,

$$C_{S5} = \begin{cases} 0.44 & (0 \leq \psi_A \leq \pi/2) \\ 0.63 & (\pi/2 \leq \psi_A \leq \pi) \end{cases} \quad (11)$$

The L_{N0} is the moment lever L_N in Eq. (9).

Figure 13 shows the comparison between the experimental results on C_N and calculated ones. In case of $L_{GA}=100\text{m}$, C_N has unique value having larger than them of the other cases. The formulation Eq. (9) with Eq. (10) has good agreement for estimating the L_N in the shielding condition.

4 ASSESSMENT OF PRESENT MODIFIED WIND FORCE ESTIMATION METHOD FOR A LNG SHIP

In order to confirm the wind shielding effect, ship manoeuvring simulation for the LNG is applied to side by side situation along with the FLNG. The MMG method is used in the simulation.

The equations are defined as follows [6, 8~10]:

$$(m + m_x)\dot{u} - (m + m_y)vr = X_{H0} + X_P + X_R + X_A$$

$$(m + m_y)\dot{v} + (m + m_x)ur = Y_H + Y_R + Y_A \quad (12)$$

$$(I_{ZZ} + J_{ZZ})\dot{r} = N_H + N_R + N_A$$

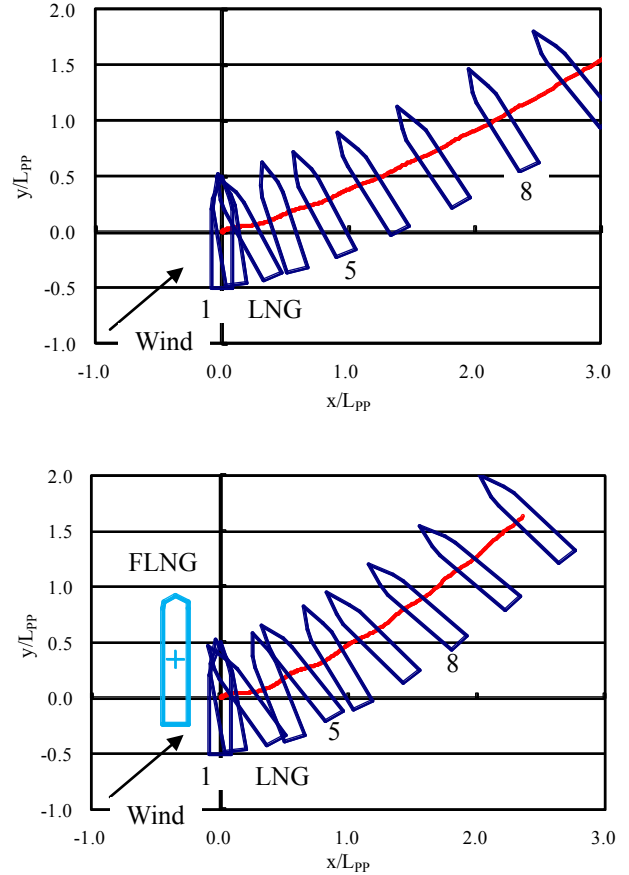


Figure 14. LNG drifting motion based on the simulation on ship manoeuvrability under strong wind ($U_A=30\text{m/s}$, $\psi_A=135\text{deg.}$, Upper; No FLNG situation, Lower; Side by side situation with FLNG, Number symbols mean in same time.).

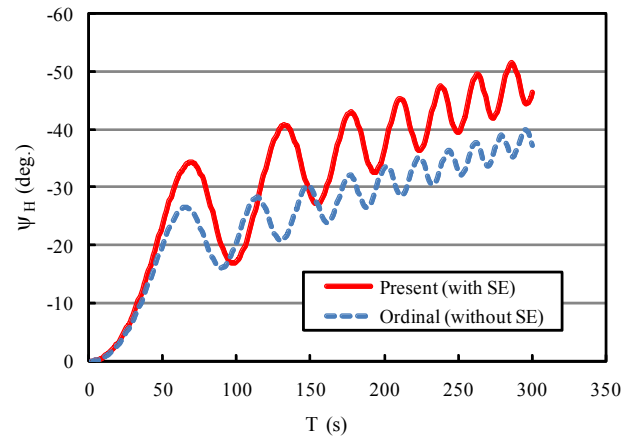


Figure 15. LNG heading angle under strong wind ($U_A=30\text{m/s}$, $\psi_A=135\text{deg.}$).

The ship mass, added mass and the yaw moment of inertia of the ship are denoted by m , I_{zz} etc. whereas the longitudinal, lateral and yaw velocities with respect to the centre of gravity of the ship are designated u , v and r . Furthermore, the external forces and moments designated X , Y , N have components arising from the hydrodynamic characteristics of the hull, the propeller generated thrust, the rudder reactive loads and the wind forces acting on the hull using the suffixions H , P , R , A . In that case, X_{H0} means calm water resistance going straight forward, and Y_H , N_H are used the experimental data for similar ship's type in the reference [11].

Figure 14 shows the LNG drifting motion based on the simulation. The ship approaches near zero speed. Then, the suffixions P , R terms have limited small values. That is, mainly Eq. (12) consists of Y_H , N_H and wind forces terms. The upper figure is the result of no FLNG situation, and the lower one is the side by side situation with FLNG in $U_A=30\text{m/s}$, $\psi_A=135\text{deg}$. Moreover, Figure 15 shows the LNG heading angle in same strong wind.

Although the calculated weather situation is severe and tough for the ship manoeuvring, the LNG heading angle shown in Figure 15 has large difference for different ship condition. For the view points of safety operation on side by side, the exact manoeuvring simulation including the shielding effect will be made into necessity in future.

5 CONCLUSIONS

Assuming the increasing opportunity of the side by side offloading operation for FLNG and LNG carrier ships, a way of estimating the wind load in that situation is proposed in this paper. This trial is one of the examples since the used ship type is one case, but the way of thinking will be able to use the actual case of the operation. The results of this paper are summarized as follows:

1. Aerodynamic characteristics for the longitudinal and lateral wind forces and the yaw, heel moment of the shielding effect is investigated and the formulation of the estimation of wind load with the effect in case of side by side operation is proposed.
2. The shielding effect is mainly calculated by the geometrical position, and the concept of the shielding area definition defined by the 4 corners of the ship form.
3. The non-dimensional parameters of the L_{GA}/L_{OA} and the L_{SA}/L_{OA} become important factors for representing the shielding effect of a ship.
4. The effect of the estimated result is shown with simulation on the mathematical modeling of a LNG ship. It is shown that the present method of estimating wind load has important role to calculate the ship manoeuvring motion in

the operational stage of the side by side operation.

REFERENCES

- [1] Eduardo Aoun Tannuri, Carlos Hakio Fucatu, Bruno Devoraes Rossin, Renata Cristina B. Montagnini, Marcos Donato Ferreira, "Wind Shielding Effects on DP System of a Shuttle Tanker", Proceedings of the 29th International Conference on Ocean, Offshore and Arctic Engineering (OMAE2010), OMAE2010-20148, China, 2010.
- [2] Arjan Voogt, "Effect of Heading Control on LNG Offloading", Proceedings of the Nineteenth International Offshore and Polar Engineering Conference (ISOPE2009), pp.199-204, Osaka, 2009.
- [3] Arjan Voogt, Hielke Brugts, "Numerical Simulations to Optimise Offshore Offloading Operations", Proceedings of 2010 Offshore Technology Conference (OTC2010), OTC20638 (2010).
- [4] Bruin, A, C, "Initial development of a method to account for wind shielding effects on a shuttle tanker during FPSO offloading", National Aerospace Laboratory NLR, NLR-CR-2003-018, Germany, 2003.
- [5] Fujiwara, T, Ueno, M, and Ikeda, Y, "A New Estimation Method of Wind Forces and Moments acting on Ships on the basis of Physical Component Models", J the Japan Society of Naval Architects and Ocean Engineers, Vol.2, pp.243-255. (in Japanese)
- [6] Fujiwara, T, Ueno, M, and Ikeda, Y, "Cruising Performance of a Large Passenger Ship in Heavy Sea", Proceedings of the Sixteenth International Offshore and Polar Engineering Conference (ISOPE2006), pp.304-311, 2006.
- [7] Fujiwara, T, Tsukada, Y, Kitamura, F, Sawada, H and Ohmatsu, S, "Experimental Investigation and Estimation on Wind Forces for a Container Ship", Proceedings of the Nineteenth International Offshore and Polar Engineering Conference (ISOPE2009), pp.555-562, 2009.
- [8] Fujiwara, T, Ueno, M, and Ikeda, Y, "Cruising performance of ships with large superstructures in heavy sea - 1st report: Added resistance induced by wind -", J the Japan Society of Naval Architects and Ocean Engineers Vol.2, pp.257-269. (in Japanese)
- [9] Tanaka, A, Yamagami, Y, Yamashita, Y and Misumi, E, "The Ship Manoeuvrability in Strong Wind", J the Kansai Society of Naval Architects, Vol.176, pp.1-10.
- [10] Kijima K, Katsuno T, Nakiri Y et al., "On the Manoeuvring Performance of a Ship with the Parameter of Loading Condition", J Society of Naval Architects of Japan, Vol.168, pp.141-148, 1990.
- [11] Obokata, J, Sasaki, N and Nagashima, J, "On the Estimation of Current Force induced on a Ship Hull by Some Model Tests", J the Kansai Society of Naval Architects, Vol.180, pp.47-57, 1981. (in Japanese)